HHS Public Access

Author manuscript

Int J Pharm. Author manuscript; available in PMC 2023 March 25.

Published in final edited form as:

Int J Pharm. 2022 March 25; 616: 121466. doi:10.1016/j.ijpharm.2022.121466.

Evaluation of Immune-Modulating Drugs for Use in Drug-eluting Microsphere Transarterial Embolization

Andrew S. Mikhail[a,¶,*], **Michal Mauda-Havakuk**[a,¶], **Ayele H. Negussie**[a], **Natalie Hong**[a], **Natalie M. Hawken**[a], **Camella J. Carlson**[a], **Joshua W. Owen**[a], **Olga Franco-Mahecha**[a], **Paul G. Wakim**[b], **Andrew L. Lewis**[c], **William F. Pritchard**[a], **John W. Karanian**[a], **Bradford J. Wood**[a]

[a]Center for Interventional Oncology, Radiology and Imaging Sciences, Clinical Center, National Institutes of Health, Bethesda, Maryland, USA

[b]Biostatistics and Clinical Epidemiology Service, National Institutes of Health Clinical Center, Bethesda, MD, USA

[c]Biocompatibles UK Ltd (a BTG International group company), Lakeview, Riverside Way, Watchmoor Park, Camberley, Surrey, GU15 3YL, UK.

[*]Corresponding author: andrew.mikhail@nih.gov; Tel. 301-435-8945 (ASM).

[¶]ASM and MMH contributed equally to this work

Author contributions

Andrew S. Mikhail: Conceptualization, Data curation; Formal analysis; Investigation; Methodology; Validation; Visualization; Writing - original draft; Writing - review & editing.
Michal Mauda-Havakuk: Conceptualization, Data curation; Formal analysis; Investigation; Methodology; Validation; Visualization; Writing - original draft; Writing - review & editing.
Ayele H. Negussie: Data curation; Investigation; Methodology; Validation; Writing - review & editing.
Natalie Hong: Data curation; Investigation; Writing - review & editing.
Natalie M. Hawken: Data curation; Investigation; Writing - review & editing.
Camella J. Carlson: Data curation; Investigation; Writing - review & editing.
Joshua W. Owen: Data curation; Investigation; Writing - review & editing.
Olga Franco-Mahecha: Data curation; Investigation; Writing - review & editing.
Paul G. Wakim: Data curation; Formal Analysis; Investigation; Writing - review & editing.
Andrew L. Lewis: Writing - Funding acquisition; Resources; review & editing.
William F. Pritchard: Project administration; Supervision; Writing - review & editing.
John W. Karanian: Project administration; Supervision; Writing - review & editing.
Bradford J. Wood: Project administration; Supervision; Writing - review & editing.

Competing interests

Professor Andrew L Lewis was an employee of Boston Scientific and Biocompatibles UK Ltd, the company sponsoring the study. BJW is the Principal Investigator for Cooperative Research & Development Agreements between NIH and the following: BTG Biocompatibles/Boston Scientific, Siemens, Philips, NVIDIA, Celsion Corp, Canon Medical, XAct Robotics. BJW and NIH are party to Material Transfer or Collaboration Agreements with: Angiodynamics, 3T Technologies, Profound Medical, Exact Imaging, Johnson and Johnson, Endocare/Healthtronics, and Medtronic. Outside the submitted work, BJW is primary inventor on 47 issued patents owned by the NIH (list available upon request), a portion of which have been licensed by NIH to Philips. BJW and NIH report a licensing agreement with Canon Medical on algorithm software with no patent. BJW is joint inventor (assigned to HHS NIH US Government) for patents and pending patents related to drug-eluting bead technology, some of which may have joint inventorships with BTG Biocompatibles/ Boston Scientific. BJW is primary inventor on patents owned by NIH in the space of drug-eluting embolic beads. The authors report no other conflicts of interest in this work.

Disclosure

The content of this manuscript does not necessarily reflect the views or policies of the U.S. Department of Health and Human Services. The mention of commercial products, their source, or their use in connection with material reported herein is not to be construed as an actual or implied endorsement of such products by the United States government.

Abstract

Cancer immunotherapy has yet to reach its full potential due in part to limited response rates and side effects inherent to systemic delivery of immune-modulating drugs. Local administration of immunotherapy using drug-eluting embolic (DEE) microspheres as drug delivery vehicles for direct infusion into tumor-feeding arteries might increase and prolong tumor drug concentrations and reduce systemic drug exposure, potentially improving the risk-to-benefit ratio of these agents. The purpose of this study was to evaluate the ability of four immune modulators affecting two different immune pathways to potentiate replication of immune cells from a woodchuck model of hepatocellular carcinoma. DSR 6434, a Toll-like receptor agonist, and BMS-202, a PD-L1 checkpoint inhibitor, induced immune cell replication and were successfully loaded into radiopaque DEE microspheres in high concentrations. Release of DSR 6434 from the DEE microspheres was rapid ($t_{99\%}$ = 0.4 h) upon submersion in a physiologic saline solution while BMS-202 demonstrated a more sustained release profile ($t_{99\%}$ = 17.9 h). These findings demonstrate the feasibility of controlled delivery of immune-modulating drugs via a local DEE microsphere delivery paradigm.

Graphical Abstract

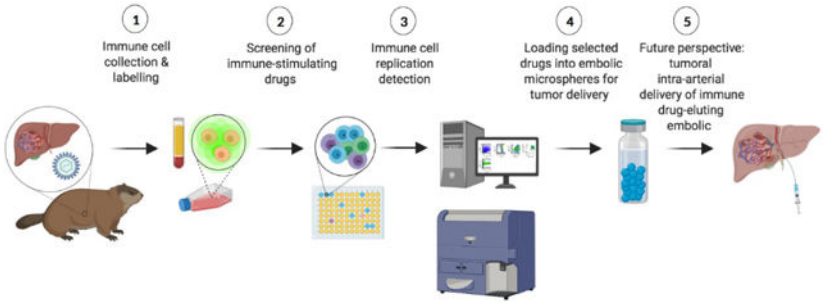

Keywords

embolization; drug-eluting beads (DEB); immunotherapy; checkpoint inhibitor; hepatocellular carcinoma; woodchuck

1.1 Introduction

Liver cancer is a leading cause of cancer-related death worldwide and has increased in incidence and mortality for decades [1]. Hepatocellular carcinoma (HCC) is the predominant form of liver cancer and typically occurs in the presence of chronic inflammation induced by human viral hepatitis, alcohol insult, or nonalcoholic fatty liver disease such as from diabetes or obesity [2]. Spontaneous tumor-specific immune responses have been observed in HCC patients including tumor antigen-specific T-cell and humoral responses that show that HCC might be susceptible to immunotherapy [3,4].

Recently, blockade of immune inhibitory pathways has demonstrated promising clinical activity leading to U.S. Food and Drug Administration approval of anti-PD-1 checkpoint inhibitors (CPI) for advanced HCC [5,6]. Chronic inflammation plays an important role

in HCC carcinogenesis, suggesting the potential to augment antitumor immune responses by activating pathways of innate immunity [7]. However, low response rates and systemic toxicities remain limiting characteristics of immunotherapy. New approaches for targeted delivery of immune-modulating drugs, such as local delivery of drug-eluting embolic (DEE) microspheres, may improve safety and broaden the number of patients that may benefit from immunotherapy.

Transarterial chemoembolization (TACE) is a minimally invasive, image-guided procedure performed by injection of chemotherapy and embolics, which occlude blood flow, into tumor-feeding arteries. Drug-eluting embolic (DEE) microspheres serve both as an embolic and a targeted drug delivery system providing intratumoral drug release and reduced systemic exposure compared to conventional systemic approaches [8,9]. TACE has been shown to promote immunogenic cell death [10] and to induce tumor-associated antigen-specific responses [11]. There is also evidence that response rates to immunotherapies may be augmented by TACE and other locoregional therapies [12]. Recently, a clinical trial combining tremelimumab, an anti-CTLA-4 monoclonal antibody, and thermal ablation or TACE in patients with advanced HCC reported objective tumor responses outside of the treated tumors as well as elevations in circulating CD4+ and CD8+ T cells, suggesting activation of systemic anti-tumor effects [13]. A number of clinical trials are ongoing to evaluate combined treatment with CPI and locoregional therapies [12].

Another promising approach to augment anti-tumor immune responses is pharmacological activation of toll-like receptor (TLR) stimulatory pathways. TLRs are pattern recognition receptors that initiate innate immune responses when exposed to microbial components or other natural or synthetic agonists. Preclinical studies have demonstrated the ability of TLR agonists to potentiate anti-tumor immune responses causing tumor regression as a monotherapy or as part of combination therapies [14–17]. However, in humans, systemic administration of TLR agonists is associated with significant toxicities and unfavorable pharmacokinetics [18]. These drugs may have more favorable therapeutic indices when administered locally or regionally via standard HCC intra-arterial therapeutic delivery paradigms.

Given their potency and known dose-limiting toxicities with systemic delivery, CPI and TLR agonists may be ideal candidates for local intra-arterial delivery using DEE microspheres. It is hypothesized that immune-modulating drugs delivered at the site of embolization may reduce off-target toxicity and better potentiate immunologic responses within the inflammatory, tumor antigen-rich microenvironment created by TACE. The viral-induced woodchuck (*Marmota monax*) HCC model recapitulates many aspects of the inflammatory and immunologic milieu of human HCC [19] and has been widely used in the study of hepatitis and antiviral agents as well as chemoprevention for HCC [20,21]. This model also possesses hyper-vascularized tumors of appropriate scale and vessel geometry to allow selective embolization with devices, drug delivery vectors and imaging systems designed for human use [22,23]. The purpose of this study was to evaluate the effects of TLR7 agonists and a small-molecule PD-L1 checkpoint inhibitor (smCPI) on peripheral mononuclear cells (PBMC) in the woodchuck HCC model, as well as to assess the loading and release characteristics of immune-modulating drug candidates from radiopaque DEE microspheres.

2.0 Materials and Methods

2.1 Animal procedures and tissue collection

This study was conducted under an animal use protocol approved by the Animal Care and Use Committee of the NIH Clinical Center. All procedures were performed in accordance with U.S. Animal Welfare Regulations. This study was also carried out in compliance with the ARRIVE guidelines. Five woodchucks (18–24 months old, 2 male, 3 female) were subjects of study (Northeastern Wildlife, Harrison, Idaho, USA). All had been infected with woodchuck hepatitis virus (WHV) (cWHV7P2a inoculum, approximately 10^9 viral particles, administered subcutaneously [24]) as newborns and were confirmed as tumor positive prior to acquisition. Animals were individually housed with 12-hour light:dark cycling to avoid potential hibernation effects, and ad libitum access to food and water. Enrichment was provided.

Woodchucks were sedated using 5% isoflurane delivered via an induction chamber followed by a mixture of pre-anesthetics (28.6 mg/kg ketamine HCl and 5 mg/kg xylazine IM) and maintained on 1–5% isoflurane and 100% oxygen (2 L/min) delivered via rabbit mask for the duration of the procedures. Woodchucks underwent imaging characterization with diagnostic ultrasound and contrast-enhanced computed tomography (CT), confirming the presence of HCC [19]. Following the imaging studies, animals were euthanized by exsanguination while under deep anesthesia for the collection of whole blood (45–60 mL) in EDTA tubes. The tubes were inverted several times in order to mix blood and EDTA homogenously to prevent coagulation.

2.2 PBMC isolation and cryopreservation

Ficoll-Paque density gradient centrifugation was used to separate PBMC immediately after collection. PBMC were washed in phosphate-buffered saline (PBS) with 1 mM EDTA. Remaining red blood cells were lysed with ACK lysis buffer and PBMC were washed in PBS-EDTA twice. PBMC were suspended in complete AIM-V (cAIM-V) media containing 10% heat-inactivated FBS, 1% penicillin (10,000 IU/mL), 1% streptomycin (10,000 μg/mL), 1% glutamine (29.3 mg/mL) and 1% HEPES buffer (1 M, pH 7.3). Cell viability was measured by trypan blue assay. Cells were cryopreserved within FBS-10% dimethylsulfoxide (DMSO) in liquid nitrogen.

2.3 PBMC culture

PBMC were removed from liquid nitrogen, thawed in a 37 °C water bath, washed twice in cAIM-V media, and incubated at 37 °C in cAIM-V media for 24 hours prior to drug exposure. PBMC ($1*10^6$ cells/mL in PBS) were incubated with 1.2 μM carboxyfluorescein succinimidyl ester (CFSE) (CellTrace™ CFSE Cell Proliferation Kit, Thermo Fisher Scientific, Waltham, MA) at 37 °C for 10 minutes and then washed twice with 10 mL of cAIM-V. CFSE-stained PBMC were cultured in triplicate at $1*10^5$ cells/well in 96-well flat bottom tissue culture plates in the presence of three different concentrations of drugs. Controls included CFSE-stained cells that were not exposed to study drugs, as well as unstained cells that were exposed to study drugs. The former were immediately fixed after staining and stored at 4 °C until flow cytometry analysis.

2.4 Drugs and controls

Concanavalin-A, 2.5 μg/mL, was used as a nonspecific stimulant of T cell proliferation. Bovine serum albumin (BSA), 2.5 μg/mL, was used as an irrelevant antigen and a negative control. Cells were incubated with gardiquimod (Enzo, Farmingdale, NY) at concentrations of 0.3, 3.0, and 30 μg/mL and DSR 6434 (Tocris Bioscience, Bristol, UK), BMS-202 (Abcam, Cambridge, MA), and GS-9620 (Advanced ChemBlocks Inc, Burlingame, CA), all at concentrations of 0.1, 1.0, and 10 μg/mL. All four drugs were solubilized in DMSO, and all samples were supplemented with equivalent concentrations of DMSO. PBMC were incubated at 37 °C for 4 days.

2.5 Immune cell replication

Cells were harvested with ice cold PBS-2 mM EDTA and washed with PBS. Triplicates were combined, transferred to a V-bottom tissue plate, and stained with blue dead cell stain for 30 minutes on ice in the dark. Cells were incubated with anti-CD3 (1:20, rat CD3 APC 1F4, BioLegend, San Diego, CA), and anti-CD4 (1:40, Hu/NHP CD4 BV480 L200, BD, San Jose, CA) for 45 minutes on ice in the dark using a 5% mixture of normal rat and normal mouse serum in FACS buffer for blocking. Woodchuck antibody for CD8 has not been established, however markers of CD3+CD4− have previously been used to identify this cell population in woodchucks [25]. Subsequently cells were washed, fixed, and analyzed by flow cytometry. Cell replication index (RI), representing the average number of divisions that cells have undergone, was analyzed using Modfit software and was standardized to negative control stimulator, BSA, in each animal.

Cell proliferation was analyzed using Modfit LT (Verity House Software, Topsham, ME). After the population of interest was gated within the viable cell population, the Cell Tracking Wizard was run to create a model from the data. The undivided cells were then set to peak 0, the number of generations was set, and the model was run. The models and raw data were checked for concordance according to peak number and location. The average number of divisions, percentage of cells in each generation, and the RI were recorded.

2.6 Pathology and immunohistochemistry

Pathology and immunohistochemistry stains were performed on banked histopathology sections from four woodchucks with HCC. These animals had been acquired and treated similarly, with sequential 5 μm thick sections from paraffin blocks of the whole liver mounted onto glass slides (Fisher Scientific, Pittsburgh, PA). For histologic examination, consecutive tissue sections were independently stained with hematoxylin and eosin (H&E), and with TLR7 antibody (rabbit polyclonal, ab113524, Abcam, Cambridge, MA). H&E-stained sections were reviewed by a veterinary pathologist and regions were identified as liver without lesions, premalignant foci, or HCC. Sections were scanned at 20X using an Aperio AT2 scanner (Leica Biosystems, Buffalo Grove, IL) into whole slide digital images. Image analysis was performed using the Cytoplasmic V2 algorithm in ImageScope version 12.4. TLR7 H-score (range: 0 to 300) was calculated automatically by multiplying the percentage of positive cells by the staining intensity. Areas of artifact such as folds and tears were excluded from analysis. For sections stained with TLR7 antibody, a nuclear stain with 3, 3-diaminobenzidine chromogen was also performed.

2.7 Drug loading into DEE microspheres

Solutions of DSR 6434 and BMS-202 were prepared in deionized water and the pH was adjusted by addition of 0.1 M hydrochloric acid (HCl) and methanesulfonic acid ($MeSO_3H$), respectively, until complete dissolution. Doxorubicin HCl (LC Laboratories, Woburn, MA) was dissolved directly in deionized water. For drug loading, radiopaque DEE microspheres, 40–90 μm in diameter (LC Bead LUMI, Biocompatibles UK Ltd, United Kingdom), were incubated with an excess of DSR 6434 or BMS-202 in solution. Doxorubicin was loaded at a concentration of 37.5 mg/mL of DEE microspheres, the typical concentration used for human DEE-TACE. To determine the amount of drug loaded, the concentration of DSR 6434 or BMS-202 in the incubation solution was measured by high performance liquid chromatography (HPLC). This was not measured during DOX loading since 100% loading efficiency at this concentration has been previously reported [26]. The HPLC system consisted of a ZORBAX Eclipse Plus C18 reversed-phase column with mobile phases consisting of acetonitrile and deionized water at ratios of 70:30 and 50:50 for DSR 6434 and BMS-202, respectively, containing 0.1% trifluoroacetic acid with 1 mL/min flow rate. The column was connected to a UV spectrophotometer with detection wavelength set at 230 nm for DSR 6434 and 240 nm for BMS-202. The area under the chromatogram peaks was converted to concentration using calibration standards of known concentrations. Drug loading was allowed to continue until no further loading was measured. DEE microspheres were then washed twice with fresh deionized water. Light transmission images of drug-loaded DEE microspheres were captured using a microscope equipped with a X5 objective and color charge-coupled device camera. Measurements of DEE microsphere diameter were performed using a minimum of 200 microspheres with a custom Matlab (ver. 2018a, Natick, MA) image segmentation algorithm.

2.8 Drug release from DEE microspheres

Fifty milliliters of normal saline (0.9 %) were poured into a glass jar and warmed to 37 °C. DEE microspheres were added to the jar and 1 mL samples were collected at regular intervals for up to 24 hours with agitation. Each sample was replaced with 1 mL fresh saline. Concentrations of DSR 6434 and BMS-202 in the collected samples were measured using HPLC, as described above for measurement of drug loading. Doxorubicin release samples were measured using the same HPLC conditions as for DSR-6434 except with mobile phase consisting of acetonitrile and deionized water (66:34) containing 0.1% trifluoroacetic acid. A fluorescence detector was used for doxorubicin with excitation and emission wavelengths of 498 and 593 nm, respectively.

2.9 Statistical analysis

Repeated-measures models were used to account for the correlation between measurements taken from the same animal. A standardized replication index (sRI) was created by dividing the RIs by their corresponding negative control RI. This ratio was analyzed to assess whether the sRIs were different from 1, as follows: three separate models were fitted to the data, one for each of three outcome measures (sRI for non-$CD3^+$ $CD3^+$, and $CD4^+$) as dependent variable, and the following independent variables: drug, drug concentration, animal, animal-by-drug interaction, and drug-by-concentration interaction.

All five independent variables were included in the model regardless of their associated p-value. Drug concentrations were defined as low (1x), middle (10x) and high (100x), corresponding to 0.3, 3.0 and 30 μg/mL for gardiquimod, and to 0.1, 1.0 and 10 μg/mL for DSR 6434, BMS-202 and GS-9620. The test of whether the sRIs were greater than 1 was based on a t-test applied to the sRIs least-squares means and their corresponding standard error, which were obtained from the model. Reported p-values are unadjusted for multiple comparisons. Responses to drugs were defined as an animal with sRI least-square mean greater than 1, and corresponding unadjusted p-value less than a threshold that varies depending on the number of statistical tests being performed and the Bonferroni general rule of thumb, i.e., 0.05 divided by the number of tests. A repeated-measures model was also used to assess TLR7 expression for different histological types. Analyses were done with SAS Version 9.4 software (SAS Institute, Inc., Cary, North Carolina). Values of drug loaded, drug released and cytoplasmic H-scores were reported as mean ± standard deviation.

3.0 Results

3.1 Immune cell replication

Flow cytometric quantification of *in vitro* woodchuck lymphocyte replication was performed for non-$CD3^+$, $CD3^+$, and $CD4^+$ sub populations. Representative results for $CD4^+$ cell replication in PBMC from one animal are shown in Fig 1. All drugs stimulated non-$CD3^+$ cell replication *in vitro* ($p \leq 0.0001$) (supplementary Table S1). DSR 6434 had the greatest overall effect (1.7181, $p<0.0001$) on cell replication in this subpopulation and also provided the most consistent response (PBMC from 4 out of 5 woodchucks) compared to all other drug and cell population tested (Figure 2D and Table S2).

On average, gardiquimod increased $CD3^+$ cell replication ($p = 0.0004$) and DSR 6434 decreased $CD3^+$ cell replication ($p < 0.0001$). $CD3^+$ cell replication was induced in PBMC from two woodchucks upon stimulation with either BMS-202 or gardiquimod (Table S3).

DSR 6434, GS-9620 and gardiquimod had no effect on $CD4^+$ cell replication. The mean sRI of BMS-202 for this cell population was 1.1443 with an unadjusted p-value of 0.0594 compared to the adjusted threshold of 0.012 (Table S1). One response was observed for the $CD4^+$ cell population upon DSR 6434 stimulation (Table S4). Overall effects and p-values for each cell sub-population are summarized in Table 1.

3.2 Immunohistochemical analysis

Regions in the pathology sections were identified as liver without lesions (n = 11), premalignant foci (n = 6), or HCC (n = 12). Immunohistochemical analysis of TLR7 expression in each area revealed downregulation of TLR7 in HCC tumors compared to premalignant tumors ($p = 0.01$) (Fig 3).

3.3 Drug loading into DEE microspheres

Based on their activity in PBMC culture, DSR 6434 and BMS-202 were selected for independent loading into DEE microspheres. Maximum loading of DSR 6434 and BMS-202 were 58.0 ± 1 and 139.7 ± 0.1 mg/mL of sedimented DEE microspheres, respectively (Table

2). No change in DEE microsphere morphology or size was observed after drug loading (Fig 4).

3.4 Drug release from DEE microspheres

The release of DSR-6434, BMS-202, and doxorubicin from DEE microspheres was assessed *in vitro* and the data fitted to a single-phase association model (Fig 5, Table 2). Release of DSR-6434 was rapid and reached a plateau in 24 minutes whereas release of BMS-202 was prolonged, occurring over a period of 17.9 hours compared to 16.7 hours for doxorubicin. The percentage of drug released, based on the model fit, was highest for DSR 6434 (Table 2).

4.0 Discussion

TACE may be modified to deliver DEE microspheres loaded with TLR agonists or checkpoint inhibitors. Delivery of immune-modulating drugs via DEE microspheres offers the potential to augment anti-tumor immune effects while mitigating toxicities commonly associated with systemic immunotherapy. In this study, three TLR7 agonists (DSR 6434, gardiquimod, and GS-9620) and a smCPI (BMS-202) containing ionizable amine groups potentially amenable to interaction with anionic DEE microspheres were selected. The immune stimulatory effects of each drug were assessed *in vitro* using PBMC from woodchucks bearing HCC tumors. We found that all drugs tested promoted innate immune cell replication, however DSR 6434 provided the greatest and most consistent proliferative effect in this cell population. DSR 6434 was also the only drug tested that resulted in promotion of CD4+ cell replication in PBMC from one woodchuck. Gardiquimod and BMS-202 had modest overall stimulatory effects in CD3+ and CD4+ cell populations, respectively. Based on these results, DSR 6434 was chosen for loading in DEE microspheres. As the only smCPI tested, BMS-202 was also evaluated for loading in DEE microspheres.

The narrow therapeutic window of TLR7 agonists upon systemic delivery make them intriguing candidates for local delivery. TLR7 is expressed primarily on plasmacytoid dendritic cells and when activated can stimulate innate immune cells that play a role in humoral and adaptive immune responses [14,27,28]. We found that TLR7 agonists, most profoundly DSR 6434, were capable of promoting innate immune cell populations in woodchuck PBMC cultures. Non-$CD3^+$ cell replication can likely be attributed to NK and B cells rather than dendritic cells due to the latter's low number in peripheral blood and low replication capacity *in vitro* [29]. TLR7 expression has been shown to be high in human hepatocytes and down regulated in HCC [30]. Similarly, in our cohort of chronically infected woodchucks, we found downregulation of TLR7 in HCC compared to premalignant foci.

PD-L1 is expressed on activated T, B, and NK cells as well as on T regulatory cells and can be exploited to generate anti-tumor responses by checkpoint blockade [31,32]. Recently, smCPI targeting the PD-1/PD-L1 pathway have been developed that may provide greater flexibility in route of administration, improved toxicity profiles, and reduced cost compared to antibody-based CPIs [33–35]. In contrast to antibody-based therapeutics, the small size and tunable chemical structures of smCPI make them ideal candidates for linkage

or loading into vectors or carriers such as DEE microspheres for transarterial delivery. We have previously reported a lack of PD-L1 expression in woodchuck HCC tumors [19]. In human HCC, the predictive value of PD-L1 expression for efficacy of PD-L1 and PD-1 inhibitors has not been established. Some patients with low expression of PD-L1 may still benefit from PD-L1 and PD-1 inhibitors [36,37].

Prior to loading in DEE microspheres, BMS-202 and DSR 6434 were converted into their salt forms in order to improve their water solubility. Protonation of amine groups (see drug chemical structures Figure S1) in the presence of an acid leads to the formation of a positive charge center that can promote drug loading by electrostatic interaction with anionic sulfonate groups in the microspheres [38,39]. Drug release occurs by ion-exchange during which the drug is displaced by positively charged ions in the elution media [40]. The strength of drug-bead electrostatic interactions and the ionic strength of the surrounding environment are important determinants of the rate of drug release [40]. Drug-drug intermolecular interactions can also affect the rate of drug release [41–43]. For amphiphilic molecules such as BMS-202, potential aggregation promoted by the hydrophobic effect may be stabilized by electrostatic interaction within the charged polymer network of the DEE microspheres, reducing the rate and extent of drug release resulting in prolonged and incomplete drug release [42,44,45]. By contrast, the rapid release of DSR 6434 suggests only weak interaction between the drug and the DEE microspheres.

The poor solubility of TLR agonists and smCPI in this study in their non-ionized forms might generally require formulation with organic solvents or surfactants for optimal intratumoral injection. Rapid clearance of these small-molecule drugs after intratumoral injection might necessitate multiple multi-focal low-dose injections throughout the tumor to achieve therapeutic spatial drug coverage. We found that high concentrations of these drugs could be loaded in DEE microspheres without the use of organic solvents. Drug-loaded DEE microspheres might also provide enhanced spatial control of targeted drug delivery as the delivery microcatheter may be advanced into the artery directly supplying the tumor. For drugs with prolonged release profiles, such as BMS-202, DEE microspheres can enable local, continuous drug delivery over an extended period of time effectively reducing peak plasma drug concentrations and increasing target tumor drug levels [9,46,47]. For fast-releasing drugs like DSR 6434, systemic exposure may approximate that of intravenous or intraarterial delivery of free drug, although high tumor drug levels resulting from localized delivery and potential reductions in drug washout following embolization may provide some benefit.

In practice, DEE microspheres are loaded with a single drug, but loading two immunomodulators into DEE microspheres is an intriguing possibility. DEE microspheres could be co-loaded with synergistic drug combinations or different single-agent microspheres could be mixed in an effort to maximize therapeutic effects. It may even be possible to load different drugs into microspheres containing different radiopacifiers that could be distinguished using dual-energy or photon-counting CT. This could permit visual confirmation of spatial distribution of multiple drug-microsphere combinations to, for example, different tumor immune microenvironments. Such microsphere-based drug delivery paradigms merit further study.

This study had several limitations towards demonstration of this novel immune-DEE paradigm. *In vitro* investigations such as immune replication of PBMC reflects several key processes in systemic immunity. Nevertheless, it does not fully capture the breadth of the *in vivo* immune response over time and its inherently multi-compartmental nature. Nor did we specifically assess the effects of immune-modulating drugs on the intratumoral immune microenvironment. The liver is a tolerogenic immune organ with inherent immune suppressive mechanisms that may be challenging to investigate *in vitro* or *in vivo* in any model. Downregulation of immune responses from chronic decades-long inflammation, as seen in human HCC, may not be fully reproduced during the shorter life span of the woodchuck, despite some hepatitis-induced similarities [19]. *In vitro* drug release from DEE microspheres may not reflect drug release *in vivo*, but rather provides insight into the relative release rates for comparison of one drug to another and to the well-studied standard clinical doxorubicin release profile, under the same controlled conditions. Finally, the limited availability of woodchuck antibodies for immunological analyses prevented a more comprehensive species-specific assessment of immune cell populations. Further, immune cell sub-populations were relatively small, which may result in variability.

In summary, this study demonstrates promotion of immune cell replication by TLR7 agonists and smCPI *in vitro* using PBMC from woodchucks chronically infected with WHV and bearing HCC tumors. These immune-modulating drugs could be loaded into and eluted from radiopaque DEE microspheres suggesting suitability of this drug-device combination for controlled local delivery of immunomodulatory agents via transcatheter embolization.

5.0 Conclusions

Loading immune-modulating drugs in radiopaque DEE microspheres was feasible and may facilitate high-dose, tumor-localized immunotherapy with the goal of minimizing systemic drug toxicity while potentiating anti-tumor immune responses. Feasibility of local immunomodulation via image-able DEE microsphere carriers loaded with smCPI or TLR agonists in the setting of HCC merits further investigation.

Supplementary Material

Refer to Web version on PubMed Central for supplementary material.

Funding:

This work was supported by the Center for Interventional Oncology in the Intramural Research Program of the National Institutes of Health (NIH) by intramural NIH Grants NIH Z01 1ZID BC011242 and CL040015. Dr. Mauda-Havakuk was supported by the Intramural Research Program of the National Institute of Biomedical Imaging and Bioengineering. NIH has a Materials Transfer Agreement with Northeastern Wildlife. The NIH and Boston Scientific Corporation (previously Biocompatibles UK Ltd) have a Cooperative Research and Development Agreement providing support for this research. NIH had control over the conduct of the study, the inclusion of any data, data analysis and interpretation, manuscript preparation, editing, and decisions on submission for publication.

References

1. Cancer Facts & Figures 2020. American Cancer Society, (2020).
2. Yang JD et al. A global view of hepatocellular carcinoma: trends, risk, prevention and management. Nat Rev Gastroenterol Hepatol. 16, 589–604, (2019). [PubMed: 31439937]

3. Mizukoshi E et al. Comparative analysis of various tumor-associated antigen-specific t-cell responses in patients with hepatocellular carcinoma. Hepatology. 53, 1206–1216, (2011). [PubMed: 21480325]
4. Korangy F et al. Spontaneous tumor-specific humoral and cellular immune responses to NY-ESO-1 in hepatocellular carcinoma. Clin Cancer Res. 10, 4332–4341, (2004). [PubMed: 15240519]
5. Finkelmeier F, Waidmann O & Trojan J Nivolumab for the treatment of hepatocellular carcinoma. Expert Rev Anticancer Ther. 18, 1169–1175, (2018). [PubMed: 30304963]
6. Zhu AX et al. Pembrolizumab in patients with advanced hepatocellular carcinoma previously treated with sorafenib (KEYNOTE-224): a non-randomised, open-label phase 2 trial. Lancet Oncol. 19, 940–952, (2018). [PubMed: 29875066]
7. Roth GS & Decaens T Liver immunotolerance and hepatocellular carcinoma: Pathophysiological mechanisms and therapeutic perspectives. Eur J Cancer. 87, 101–112, (2017). [PubMed: 29145036]
8. Varela M et al. Chemoembolization of hepatocellular carcinoma with drug eluting beads: efficacy and doxorubicin pharmacokinetics. J Hepatol. 46, 474–481, (2007). [PubMed: 17239480]
9. Poon RT et al. A phase I/II trial of chemoembolization for hepatocellular carcinoma using a novel intra-arterial drug-eluting bead. Clin Gastroenterol Hepatol. 5, 1100–1108, (2007). [PubMed: 17627902]
10. Kohles N, Nagel D, Jungst D, Stieber P & Holdenrieder S Predictive value of immunogenic cell death biomarkers HMGB1, sRAGE, and DNase in liver cancer patients receiving transarterial chemoembolization therapy. Tumour Biol. 33, 2401–2409, (2012). [PubMed: 22965881]
11. Ayaru L et al. Unmasking of alpha-fetoprotein-specific CD4(+) T cell responses in hepatocellular carcinoma patients undergoing embolization. J Immunol. 178, 1914–1922, (2007). [PubMed: 17237442]
12. Greten TF, Mauda-Havakuk M, Heinrich B, Korangy F & Wood BJ Combined locoregional-immunotherapy for liver cancer. J Hepatol. 70, 999–1007, (2019). [PubMed: 30738077]
13. Duffy AG et al. Tremelimumab in combination with ablation in patients with advanced hepatocellular carcinoma. J Hepatol. 66, 545–551, (2017). [PubMed: 27816492]
14. Zhou Z, Yu X, Zhang J, Tian Z & Zhang C TLR7/8 agonists promote NK-DC cross-talk to enhance NK cell anti-tumor effects in hepatocellular carcinoma. Cancer Lett. 369, 298–306, (2015). [PubMed: 26433159]
15. Rodell CB et al. TLR7/8-agonist-loaded nanoparticles promote the polarization of tumour-associated macrophages to enhance cancer immunotherapy. Nat Biomed Eng. 2, 578–588, (2018). [PubMed: 31015631]
16. Mullins SR et al. Intratumoral immunotherapy with TLR7/8 agonist MEDI9197 modulates the tumor microenvironment leading to enhanced activity when combined with other immunotherapies. J Immunother Cancer. 7, 244, (2019). [PubMed: 31511088]
17. Zhu J et al. Local administration of a novel Toll-like receptor 7 agonist in combination with doxorubicin induces durable tumouricidal effects in a murine model of T cell lymphoma. J Hematol Oncol. 8, 21, (2015). [PubMed: 25887995]
18. Engel AL, Holt GE & Lu H The pharmacokinetics of Toll-like receptor agonists and the impact on the immune system. Expert Rev Clin Pharmacol. 4, 275–289, (2011). [PubMed: 21643519]
19. Mauda-Havakuk M et al. Imaging, Pathology, and Immune Correlates in the Woodchuck Hepatic Tumor Model. J Hepatocell Carcinoma. 8, 71–83, (2021). [PubMed: 33728278]
20. Tennant BC et al. Hepatocellular carcinoma in the woodchuck model of hepatitis B virus infection. Gastroenterology. 127, S283–S293, (2004). [PubMed: 15508096]
21. Roggendorf M, Kosinska AD, Liu J & Lu M The woodchuck, a nonprimate model for immunopathogenesis and therapeutic immunomodulation in chronic hepatitis B virus infection. Cold Spring Harb Perspect Med. 5, (2015).
22. Pritchard WF et al. Transarterial chemoembolization in a woodchuck model of hepatocellular carcinoma. J Vasc Interv Radiol. 31, 812–819.e811, (2020). [PubMed: 32107125]
23. Wilkins LR et al. The use of the woodchuck as an animal model for evaluation of transarterial embolization. J Vasc Interv Radiol. 28, 1467–1471, (2017). [PubMed: 28941521]

24. Fletcher SP et al. Intrahepatic Transcriptional Signature Associated with Response to Interferon-alpha Treatment in the Woodchuck Model of Chronic Hepatitis B. PLoS Pathog. 11, e1005103, (2015). [PubMed: 26352406]
25. Balsitis S et al. Safety and efficacy of anti-PD-L1 therapy in the woodchuck model of HBV infection. PLoS One. 13, e0190058, (2018). [PubMed: 29444087]
26. Lewis AL et al. Handling and performance characteristics of a new small caliber radiopaque embolic microsphere. J Biomed Mater Res B Appl Biomater. 108, 2878–2888, (2020). [PubMed: 32578348]
27. Boni C et al. TLR7 Agonist Increases Responses of Hepatitis B Virus-Specific T Cells and Natural Killer Cells in Patients With Chronic Hepatitis B Treated With Nucleos(T)Ide Analogues. Gastroenterology. 154, 1764–1777 e1767, (2018). [PubMed: 29378197]
28. Berggren O, Pucholt P, Amcoff C, Ronnblom L & Eloranta ML Activation of plasmacytoid dendritic cells and B cells with two structurally different Toll-like receptor 7 agonists. Scand J Immunol, e12880, (2020). [PubMed: 32219875]
29. Clanchy FI, Holloway AC, Lari R, Cameron PU & Hamilton JA Detection and properties of the human proliferative monocyte subpopulation. J Leukoc Biol. 79, 757–766, (2006). [PubMed: 16434691]
30. Lin KJ et al. Down-regulation of Toll-like receptor 7 expression in hepatitis-virus-related human hepatocellular carcinoma. Hum Pathol. 44, 534–541, (2013). [PubMed: 23069256]
31. Hollern DP et al. B Cells and T Follicular Helper Cells Mediate Response to Checkpoint Inhibitors in High Mutation Burden Mouse Models of Breast Cancer. Cell. 179, 1191–1206 e21, (2019). [PubMed: 31730857]
32. Boussiotis VA Molecular and Biochemical Aspects of the PD-1 Checkpoint Pathway. N Engl J Med. 375, 1767–1778, (2016). [PubMed: 27806234]
33. Sasikumar PG & Ramachandra M Small-molecule immune checkpoint inhibitors targeting PD-1/PD-L1 and other emerging checkpoint pathways. BioDrugs. 32, 481–497, (2018). [PubMed: 30168070]
34. Guzik K et al. Development of the inhibitors that target the PD-1/PD-L1 interaction-a brief look at progress on small molecules, peptides and macrocycles. Molecules. 24, 2071, (2019).
35. Zak KM et al. Structural basis for small molecule targeting of the programmed death ligand 1 (PD-L1). Oncotarget. 7, 30323–30335, (2016). [PubMed: 27083005]
36. Zhu AX et al. Pembrolizumab in patients with advanced hepatocellular carcinoma previously treated with sorafenib (KEYNOTE-224): a non-randomised, open-label phase 2 trial. Lancet Oncol. 19, 940–952, (2018). [PubMed: 29875066]
37. Sangro B et al. Association of inflammatory biomarkers with clinical outcomes in nivolumab-treated patients with advanced hepatocellular carcinoma. J Hepatol. 73, 1460–1469, (2020). [PubMed: 32710922]
38. Lewis AL DC Bead: a major development in the toolbox for the interventional oncologist. Expert Rev Med Devices. 6, 389–400, (2009). [PubMed: 19572794]
39. de Baere T et al. An in vitro evaluation of four types of drug-eluting microspheres loaded with doxorubicin. J Vasc Interv Radiol. 27, 1425–1431, (2016). [PubMed: 27402527]
40. Gonzalez MV et al. Doxorubicin eluting beads-2: methods for evaluating drug elution and in-vitro:in-vivo correlation. J Mater Sci Mater Med. 19, 767–775, (2008). [PubMed: 17653626]
41. Biondi M, Fusco S, Lewis AL & Netti PA New insights into the mechanisms of the interactions between doxorubicin and the ion-exchange hydrogel DC Bead™ for use in transarterial chemoembolization (TACE). J Biomater Sci Polym Ed. 23, 333–354, (2012). [PubMed: 21255482]
42. Ahnfelt E, Sjögren E, Hansson P & Lennernäs H In vitro release mechanisms of doxorubicin from a clinical bead drug-delivery system. J Pharm Sci. 105, 3387–3398, (2016). [PubMed: 27663384]
43. Fülöp Z, Gref R & Loftsson T A permeation method for detection of self-aggregation of doxorubicin in aqueous environment. Int J Pharm. 454, 559–561, (2013). [PubMed: 23850794]
44. Ahnfelt E et al. Single bead investigation of a clinical drug delivery system – A novel release mechanism. J Control Release. 292, 235–247, (2018). [PubMed: 30419268]
45. Hansson P Surfactant Self-Assembly in Oppositely Charged Polymer Networks. Theory. J Phys Chem B. 113, 12903–12915, (2009). [PubMed: 19728696]

46. Hong K et al. New intra-arterial drug delivery system for the treatment of liver cancer: preclinical assessment in a rabbit model of liver cancer. Clin Cancer Res. 12, 2563–2567, (2006). [PubMed: 16638866]

47. Lewis AL et al. Feasibility, safety and pharmacokinetic study of hepatic administration of drug-eluting beads loaded with irinotecan (DEBIRI) followed by intravenous administration of irinotecan in a porcine model. J Mater Sci Mater Med. 24, 115–127, (2013). [PubMed: 23015264]

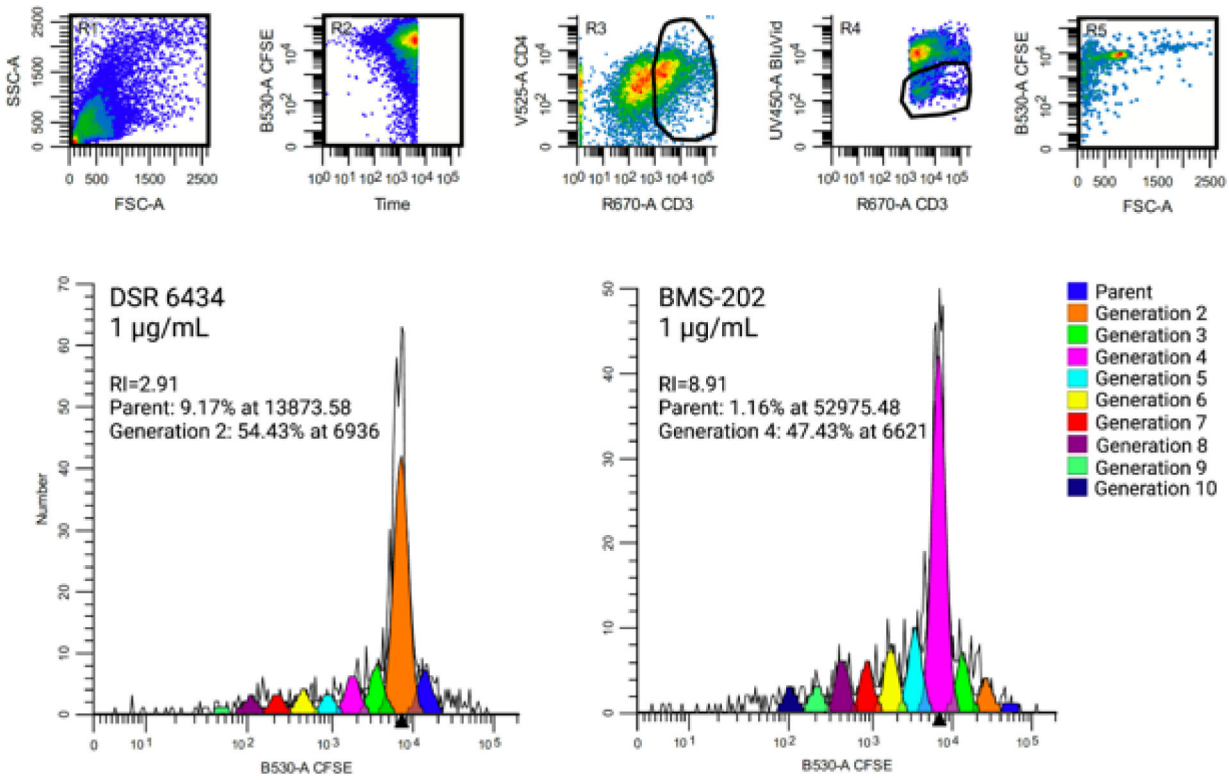

Fig 1. Flow cytometric quantification of woodchuck CD4^{+} lymphocyte replication.

CD4^{+} Lymphocyte generations and calculated replication index (RI) for PBMC from one woodchuck stimulated with DSR 6434 or BMS-202 both at a concentration of 1 µg/mL. Gating strategy is provided in the upper panel. Forward and side scatter plot of PBMC is presented in R1. CFSE replication profile was generated by gating on cells that were CD3^{pos} CD4^{pos} (R3), viable (R4) and CFSE^{pos} (R5).

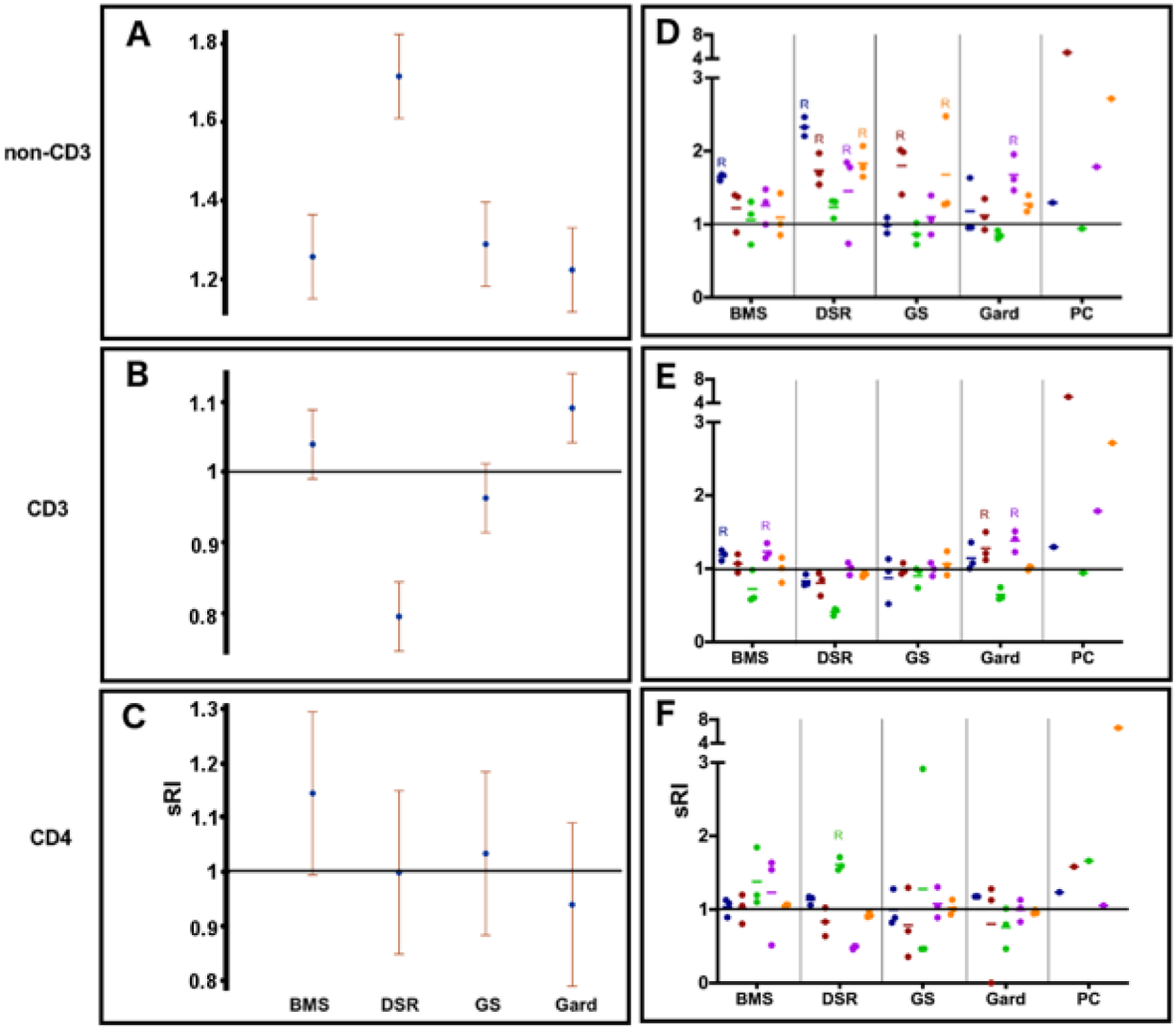

Fig 2. The effect of immune-modulating drugs on lymphocyte replication.

(A-C) The sRI is presented for all drugs for non-CD3$^+$ (A), CD3 (B), and CD4$^+$ (C) sub-populations. P-values are summarized in Table S1 and Table S2. (D-F) PBMC from 5 animals (each donor is color coded) were cultured with three 10-fold serial concentrations of immune-modulating drugs (BMS-202, DSR 6434, GS-9620: 0.1–10 μg/mL; and gardiquimod: 0.3–30 μg/mL, 3 dots per color represent 3 concentrations per donor) for 4 days. RIs were calculated for non-CD3$^+$ (D), CD3$^+$ (E), and CD4$^+$ (F) cell populations. BMS = BMS-202; DSR = DSR 6434; GS = GS-9620; Gard = gardiquimod; PC = positive control.

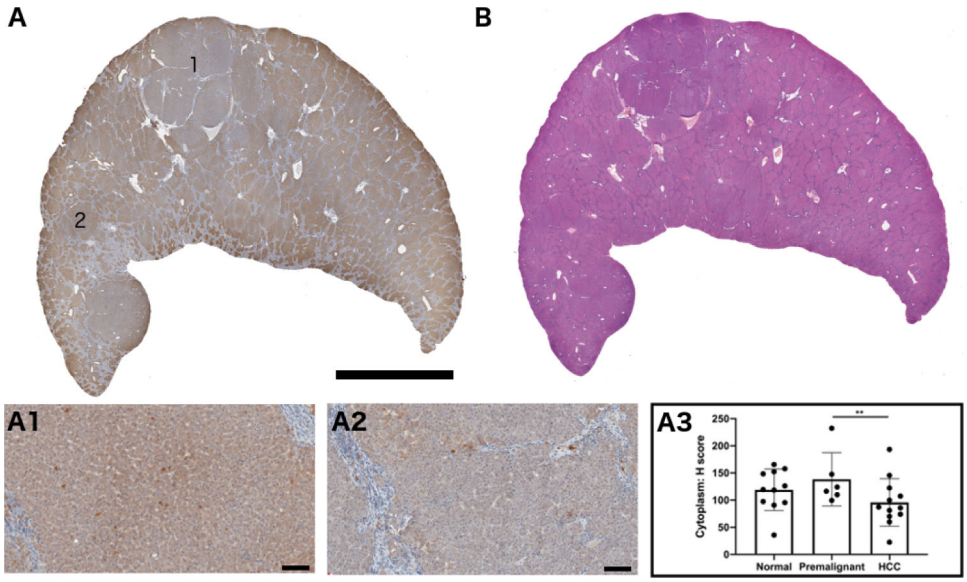

Fig 3. TLR7 expression in woodchuck hepatic tumors.

(A) Whole section stained for TLR7 expression. Region 1 shows TLR expression within an HCC tumor and region 2 represents TLR expression within a premalignant focus. (A1) Magnification of region 1 and (A2) region 2. (A3) Quantification of TLR7 expression in 11 normal hepatic tissues (no tumor), 6 premalignant foci, and 12 HCC tumors (** p = 0.01). (B) H&E-stained section corresponding to section (A). Scale bar is 2 cm for A and B and 100 μm for A1 and A2.

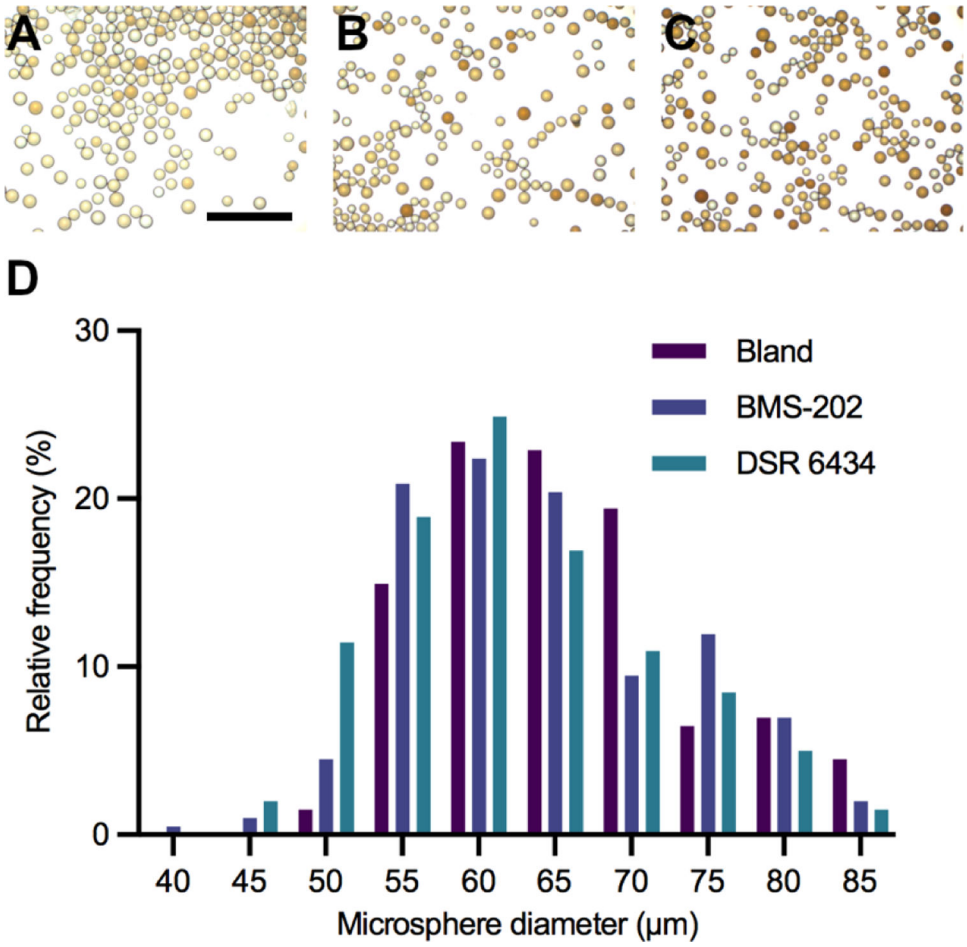

Figure 4. Morphology and size distribution of radiopaque DEE microspheres.

Light microscope images of DEE microspheres before (A) and after loading with (B) DSR 6434 or (C) BMS-202. Scale bar represents 500 μm. (D) Size distribution of bland (no drug) and drug-loaded DEE microspheres.

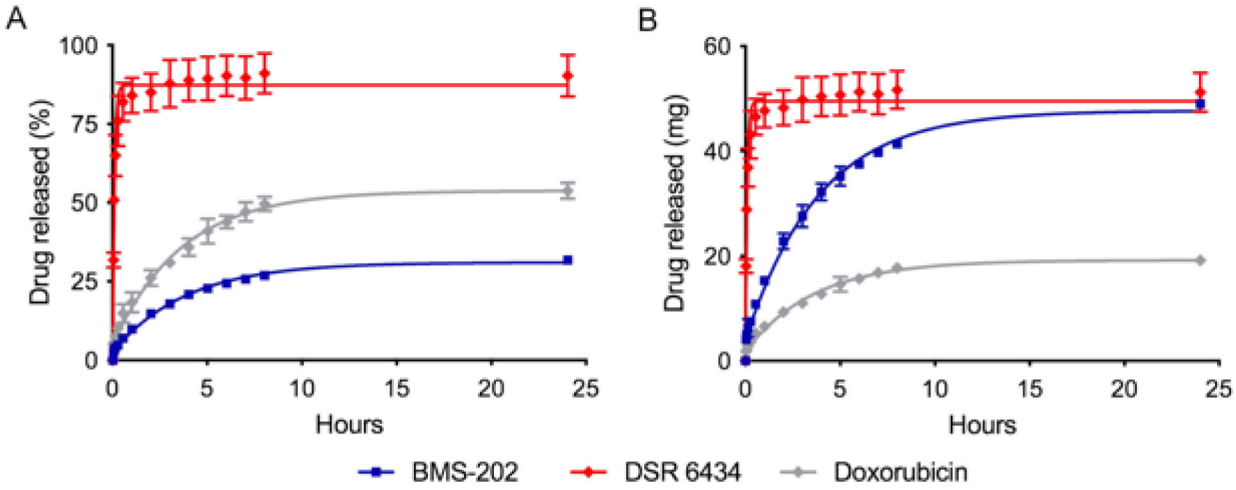

Fig 5. Release of DSR 6434, BMS-202, and doxorubicin from DEE microspheres *in vitro*.

A) The amount released as a percent of the total drug loaded in DEE microspheres. B) The amount released in mg drug/mL of DEE microspheres. Data points are fitted using a first-order kinetics model.

Table 1.

Summary of P-values for Overall Effects from Mixed Models.*

Stain	Total # of observations analyzed	p-value for overall drug effect	p-value for overall drug concentration effect	p-value for drug-by-drug concentration interaction	p-value for animal effect	p-value for animal-by-drug interaction
Non-$CD3^+$	60	<.0001	0.5776	0.0030	<.0001	<.0001
$CD3^+$	60	<.0001	0.0200	0.0018	<.0001	<.0001
$CD4^+$	60	0.2790	0.0250	0.0176	0.0173	0.0469

* P-values are unadjusted for multiple comparisons. As a general rule of thumb, p-values less than 0.01 (= 0.05/5 tests) are considered as reflecting evidence of an effect.

Table 2.

Drug Loading and Release (based on model fit) from DEE Microspheres.

Compound	Drug loaded (mg) per mL of DEE microspheres	Total drug eluted (mg) per mL of DEE microsphere	Percent of drug eluted	t_{50} (h)[a]	t_{99} (h)[a]
DSR 6434	58.0 ± 1	49.5	87.3	0.06	0.4
BMS-202	139.7 ± 0.1	47.7	31.0	2.7	17.9
DOX	37.5 [b]	19.2	53.8	2.5	16.7

DEE: Drug-eluting embolic.

[a] t_{50} and t_{99} represent the amount of time, in hours, to reach 50% and 99% drug release, respectively, relative to the total amount of drug released, based on the model fits.

[b] 37.5 mg/mL of DEE microspheres is the typical loading concentration used in humans